A Topographical Relationship Between Visual Field Defects and Optic Radiation Changes in Glaucoma

Megha Kaushik,[1] Stuart L. Graham,[1,2] Chenyu Wang,[3] and Alexander Klistorner[1,2]

[1]Save Sight Institute, University of Sydney, Sydney, New South Wales, Australia
[2]Australian School of Advanced Medicine, Macquarie University, Sydney, New South Wales, Australia
[3]Brain and Mind Research Institute, University of Sydney, Sydney, New South Wales, Australia

Correspondence: Megha Kaushik, Save Sight Institute, 8 Macquarie Street, Sydney, New South Wales, 2000, Australia; megha.ka@gmail.com.

Submitted: May 3, 2014
Accepted: July 31, 2014

Citation: Kaushik M, Graham SL, Wang C, Klistorner A. A topographical relationship between visual field defects and optic radiation changes in glaucoma. *Invest Ophthalmol Vis Sci*. 2014;55:5770–5775. DOI:10.1167/iovs.14-14733

Purpose. To investigate the topographic relationship between glaucomatous retinal ganglion cell loss and changes in the optic radiation (OR) using diffusion tensor imaging (DTI).

Methods. A cross-sectional study was completed on nine patients with primary open angle glaucoma and nine age- and sex-matched controls. Glaucoma patients with binocular, symmetrical superior, or inferior visual hemifield defects were selected. A comparative DTI analysis was conducted between OR fibers connected to the affected and unaffected visual hemifield in the glaucoma group and corresponding OR in the control group.

Results. There was a significantly lower number of fiber bundles in the affected OR compared with unaffected OR and controls ($P < 0.01$). Radial diffusivity was similar between the affected and unaffected OR ($P = 0.39$), but higher in both groups compared with controls ($P < 0.01$). There was no difference in axial diffusivity among all groups. As a consequence, fractional anisotropy was lower and mean diffusivity was higher in the affected and unaffected OR compared with controls.

Conclusions. A significant loss of OR fibers connected to the severely damaged part of the optic nerve head, but not the fibers connected to the relatively spared retinal hemifield shows a direct relationship between retinal neuronal damage and functionally connected OR fibers in glaucoma. However, OR fibers connected to the relatively preserved visual hemifield in the glaucoma subjects still showed changes in radial diffusivity compared with controls, suggesting possible early dysfunction. Our results support the notion that glaucoma is a neurodegenerative disease involving the posterior visual pathway.

Keywords: glaucoma, diffusion tensor imaging, transsynaptic degeneration, optic radiation

Glaucoma is the third major cause of blindness globally, creating a burden of 4.7 million disability-adjusted life years.[1,2] Early diagnosis is important, as significant loss of retinal ganglion cells (RGCs) and their axons occurs before demonstrable visual field defects. The understanding of glaucoma is evolving from a pure ophthalmic condition characterized by optic neuropathy and RGC loss to a multifactorial neurodegenerative disease involving the entire visual pathway.[3] Transsynaptic degeneration has been suggested in neurodegenerative diseases like glaucoma and multiple sclerosis, yet is not definitive, as primary neurodegeneration is also a possibility.

Many studies examining the pathophysiology of changes in the posterior visual pathway in glaucoma have been postmortem or experimental.[4–6] However, advancements in magnetic resonance imaging (MRI) have been a promising avenue for understanding widespread neurodegeneration in this disease in vivo. In particular, diffusion tensor imaging (DTI) has recently been used to examine the retro-geniculate pathway in glaucoma patients.[7–13] Diffusion tensor imaging detects the Brownian motion of water molecules inside white matter tissue. The anisotropic nature of this motion allows the reconstruction of major white matter tracts, including the optic radiation (OR). Disease can alter the magnitude and direction of this movement. In glaucoma, changes in OR diffusivity have been identified and reduced rarefaction of the OR was reported recently to suggest a loss in OR fibers.[14]

Although correlation between the overall degree of glaucomatous retinal damage and changes in DTI indices of the OR has been the subject of several studies, topographical correspondence between the two has not previously been examined. Therefore, this study aimed to investigate the topographic relationship between the severity of RGC loss and changes in the posterior visual pathway in glaucoma by analyzing the DTI-reconstructed OR.

Methods

Ethics Statement

Approval was obtained from the Human Research Ethics Committee of the University of Sydney (number 2013/106) and written informed consent was obtained from all participants. The study adheres to the tenets of the Declaration of Helsinki.

Participant Selection

A cross-sectional study was completed on nine patients with primary open angle glaucoma (POAG) as diagnosed by an

ophthalmologist specialized in glaucoma. By reviewing glaucoma clinic files at random, patients were selected based on their most current Humphrey visual fields test. Patients were included if they had a binocular, symmetrical superior or inferior hemifield altitudinal defect with the fellow hemifield relatively well preserved based on their pattern deviation plot. To objectively identify patients with severe binocular hemifield defects, the difference between the unaffected and affected hemifield sensitivity (in decibels) had to be more than 3:1. There were six patients who met the criteria with bilateral superior hemifield defects and three patients with bilateral inferior hemifield defects. Exclusion criteria included concomitant ocular or neurological disease or high refractive error outside the range of ±4 diopters (D). Patients unable to undergo MRI were also excluded due to implantation of metal or psychological reasons.

The glaucoma group was compared with nine age- and sex-matched healthy controls who were known to the research staff at Save Sight Institute. These controls were included based on criteria of 6/6 vision and no history of ocular, neurological, or autoimmune disease; diabetes mellitus; or high refractive error (outside of the range between ±4 D).

Optical Coherence Tomography (OCT)

The glaucoma group underwent OCT using Spectralis HRA-OCT (Heidelberg Engineering, Heidelberg, Germany). Both eyes were scanned. Global, superior, and inferior retinal nerve fiber layer (RNFL) thickness were assessed using the axonal RNFL protocol around the optic disc. Only scans that were of good quality defined by signal strength greater than 25, good centration, and uniform brightness were used. One hundred scans were averaged to produce a resolution of 1536 pixels.

Magnetic Resonance Image Acquisition

All study participants underwent MRI brain scans at the Brain and Mind Research Institute on an MR750 3-Tesla scanner with an 8-channel head-coil (GE Medical Systems, Milwaukee, WI, USA). T1-weighted imaging with 1-mm isotropic resolution was obtained to allow anatomical localization. A customized sequence was used with the following image parameters: axial acquisition, field of view (FOV) = 240 mm^2, acquisition matrix (frequency × phase) = 240 × 240, phase encoding direction: left to right, echo time (TE) = 2.612 seconds, repetition time (TR) = 6.98 seconds, pixel bandwidth 325.547 Hz/pixel, and slice thickness = 1 mm. Whole-brain DTI was obtained to perform tractography. The protocol used 64 gradient directions DTI and the following parameters: axial acquisition, FOV = 256 mm^2, acquisition matrix (frequency × phase) = 128 × 128, phase encoding direction: anterior to posterior, TE = 84.3 seconds, TR = 8325 seconds, pixel bandwidth = 1953.12 Hz/pixel, and slice thickness = 2 mm. Two images without gradient loading (b0 s/mm^2) were acquired before the acquisition of 64 images (each containing 68 slices) with uniform gradient loading (b = 1000s/mm^2). T2-weighted fluid-attenuated inversion recovery (FLAIR) CUBE imaging was obtained to exclude confounding cerebral lesions using the following parameters: axial acquisition, FOV = 220 mm^2, acquisition matrix (frequency × phase) = 320 × 256, phase encoding direction: left to right, TE = 132.396 seconds, TR = 10,000 seconds, pixel bandwidth 325.547 Hz/pixel, and slice thickness = 5 mm.

Magnetic Resonance Image Analysis

The investigators were blinded for MRI analysis. The DICOM format of the MRI images was converted to NIFTI using dcm2nii software (McCausland Center for Brain Imaging, Columbia, SC, USA).

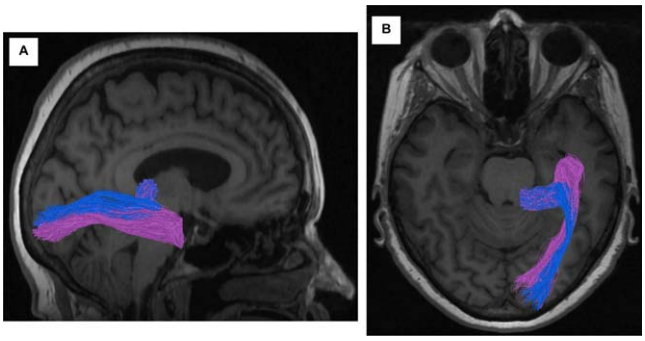

FIGURE 1. Division of the optic radiation into superior (*blue*) and inferior (*purple*) fibers based on Meyer's loop. (**A**) Sagittal view. (**B**) Axial view.

Probabilistic tractography to identify the OR was performed on all participants.[15,16] Using Mr Vista software (Stanford University, Stanford, CA, USA), DTI tensor fitting was performed. This involved computation of a non–diffusion-weighted image B0, Eddy-current correction, coregistration of DTI data to T1-weighted volumetric imaging, and fitting the tensor model. The optic chiasm was identified on the T1-weighted image. A region of interest (ROI) was placed on the optic chiasm and through deterministic tractography the right and left optic tracts were generated. Tractography for all subjects was set within the following fiber-tracking parameters: an angle threshold of 180°, fractional anisotropy 0.05, and algorithm 3. Any inaccurate fibers (i.e., fibers situated outside of the known OR position or fibers crossing into the opposite hemisphere) were removed manually using Quench software (part of the MrDiffusion package from http://sirl.stanford.edu/software; Stanford University). Based on the optic tract fiber end points, the lateral geniculate nucleus (LGN) was localized and saved as a 7-mm ROI. This large ROI was used to ensure the entire LGN was encapsulated. The calcarine cortex in the ipsilateral hemisphere was manually mapped.

ConTrack software (part of the MrDiffusion package) on the Linux 64-bit operating system was used to identify the OR between the LGN and ipsilateral calcarine cortex via a probabilistic fiber-tracking algorithm. Initially, 70,000 fibers were generated; however, the 30,000 best-scored fibers were automatically selected. Inaccuracies in the OR fibers were cleaned manually using Quench (part of the MrDiffusion package).

Based on projection to the superior or inferior calcarine cortex, the OR fibers were separated manually into tracts subserving the superior hemifield or inferior hemifield of the visual field, as shown in Figure 1. In agreement with a superior hemifield visual field defect, the inferior OR tract was labeled "affected" and superior tract was labeled as "unaffected" in six glaucoma patients and vice versa in the remaining three patients. Knowledge that fibers in Meyer's Loop represent the inferior visual field helped with the division.[16] Meyer's loop was identifiable in all subjects. To account for any possible differences in the superior and inferior OR fibers in the healthy controls, we only included either the superior or inferior OR division for each control in the same ratio as the glaucoma group (i.e., three superior and six inferior OR divisions). For consistency, the right OR was selected in all patients and controls except for one patient in whom the calcarine cortex was better defined in the left hemisphere. A previous study of healthy controls showed no difference in DTI metrics between the right and left OR.[17]

Investigative Ophthalmology & Visual Science

TABLE. Average Diffusion Tensor Indices of the OR in Glaucoma and Control Participants

Group	OR Division	Fiber Number	FA	MD	AD	RD
Glaucoma	Affected OR	3392 ± 4059	0.44 ± 0.03	0.93 ± 0.06	1.39 ± 0.08	0.69 ± 0.06
	Unaffected OR	12911 ± 7483	0.45 ± 0.02	0.91 ± 0.06	1.40 ± 0.08	0.67 ± 0.05
Controls	Superior OR	14106 ± 5010	0.51 ± 0.02	0.81 ± 0.02	1.32 ± 0.04	0.56 ± 0.02
	Inferior OR	10926 ± 1413	0.51 ± 0.02	0.84 ± 0.04	1.37 ± 0.06	0.58 ± 0.04
	Average of 3 superior and 6 inferior OR divisions	11279 ± 3102	0.51 ± 0.02	0.83 ± 0.04	1.35 ± 0.07	0.57 ± 0.04

Affected OR, optic radiation fibers connected to the affected visual field; unaffected OR, optic radiation fibers connected to the unaffected visual field; fiber number, number of fiber tract bundles.

The superior and inferior OR created in Quench were saved separately, which allowed the total number of fiber bundles and DTI indices to be automatically calculated for each OR division using MrVista. These diffusion indices are generated from the eigenvectors of each voxel, which have three eigenvalues and measure the directional diffusion of water molecules. Radial diffusivity (RD) comprises two eigenvalues (λ_2 and λ_3) to assess movement perpendicular to axons, whereas axial diffusivity (AD) is the principal eigenvalue (λ_1) for parallel movement. Mean diffusivity (MD) assesses the spread of diffusion by averaging all three eigenvalues. Anisotropy describes the direction of diffusivity of water molecules and fractional anisotropy (FA) is calculated from the ratio of AD and RD.

Statistical Analysis

Statistical analysis was conducted using SPSS Statistics 21.0.0 (IBM, New York, NY, USA). The means and SD of means were calculated. Multiple groups were compared using ANOVA with Bonferroni adjustment; P values less than 0.05 were considered statistically significant.

RESULTS

We recruited nine patients with POAG with a symmetrical severe superior or inferior altitudinal visual field defect. The mean age for the glaucoma group was 69 (range, 60–86). There were four males and five females. For the control group, nine participants were selected who had an average age of 68 (range, 45–85) and the ratio of males to females was 3:6. No participant had evidence of lesions or infarction on T1 or T2 FLAIR MRI.

Of the nine glaucoma patients, three had inferior bilateral altitudinal visual field defects and the remaining six had superior bilateral hemifield defects. The best corrected logMAR visual acuity for these patients was 0.35 in the left eye and 0.29 in the right eye. The affected hemifield had a lower average absolute threshold (right eye 3 db, left eye 4 db) compared with the relatively spared hemifield (right eye 21db, left eye 19 db), $P < 0.001$. In both eyes, the average RNFL thickness was significantly lower in the region corresponding to the affected visual hemifield (right eye: 50 ± 17 μm, left eye: 49 ± 18 μm) in comparison with the relatively spared region of RNFL (right eye: 89 ± 21 μm, left eye: 82 ± 25 μm), $P < 0.001$.

A comparative analysis was conducted between the "affected" and "unaffected" OR in the glaucoma group and OR of the control group (the superior OR of three controls and inferior OR of six controls). The average number of fiber bundles, anisotropy, and diffusivity for the OR of each group are shown in the Table and Figure 2. For consistency, only the right OR of each participant was analyzed.

There was a significantly lower number of fiber bundles in the glaucoma-affected OR group compared with the unaffected OR ($P = 0.001$) and controls ($P = 0.003$), but no difference in the number of fiber bundles between the unaffected OR and control groups ($P > 0.05$).

Analysis of variance performed among the three groups demonstrated a significant difference in RD ($P < 0.001$, ANOVA). Post hoc comparison showed that RD was higher in the glaucoma OR than the controls. RD was significantly higher in the unaffected OR of the glaucoma group compared with the controls ($P = 0.002$) and the difference was even larger between the affected OR and controls ($P < 0.001$). However, the increase in RD was similar in both the affected and unaffected OR glaucoma groups ($P = 0.39$). In contrast, ANOVA for AD demonstrated no significant difference among any of the three groups ($P = 0.80$, ANOVA).

As a result of diffusivity changes (i.e., increased RD and stable AD), FA was significantly reduced in the two glaucoma OR groups compared with the control group ($P \leq 0.01$ for both comparisons). The reduction in FA was similar between both glaucoma groups ($P = 0.23$). Mean diffusivity, on the other hand, increased in both glaucoma groups compared with the control OR (affected OR $P = 0.005$; unaffected OR $P = 0.04$). This increase was of similar magnitude between the affected and unaffected OR glaucoma groups ($P > 0.05$).

DISCUSSION

Glaucoma is characterized by the primary loss of RGCs, but experimental and human studies provide evidence of more extensive damage of the visual system.[4,18–20] Provided that primary damage in glaucoma occurs at the level of the RGC, spread of pathological changes to LGN neurons and beyond would require transsynaptic degeneration.

The visual system is a unique model to study transsynaptic degeneration because it comprises a chain of hierarchically organized and synaptically linked neurons that maintain strong topographic connectivity. This provides an opportunity to study the effect of primary pathological damage at one level of the visual system and secondary degeneration on neighboring levels. In addition, as a result of recent technological advances, the visual system has become accessible to in vivo structural and functional analysis. Thus, primary glaucomatous loss of RGCs and their axons can be assessed functionally by threshold perimetry and structurally by measuring RNFL and RGC layer thickness using OCT. Secondary changes in functional and structural integrity of neighboring LGN neurons can be examined by performing tractography and measuring diffusion properties of the OR.

Taking advantage of this technology, the current study investigated the topographic correspondence between glaucomatous loss of RGCs and MRI-determined changes in the OR. For this purpose, patients with a binocular hemifield loss of RGCs were examined. Specifically, patients with advance binocular loss in the superior or inferior visual hemifield ("affected" hemifield) and relatively preserved fellow hemifield ("unaffected" hemifield) were selected. Based on projection of OR fibers to the superior or inferior calcarine cortex, OR fibers

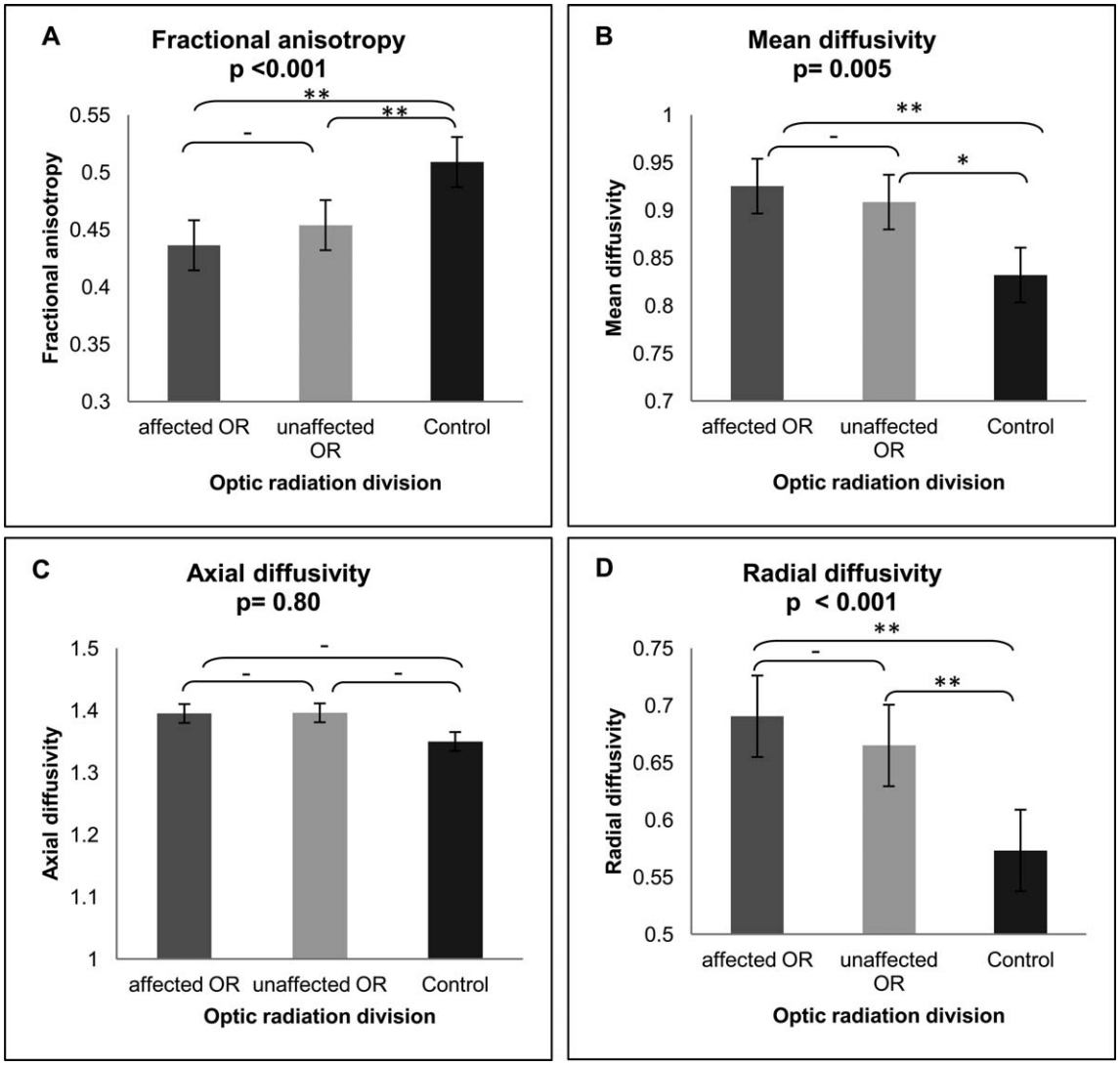

FIGURE 2. Comparison of the diffusion tensor indices of the optic radiation divisions of the glaucoma group (affected and unaffected OR) and control group. (**A**) FA. (**B**) MD. (**C**) AD. (**D**) RD. $^{**}P < 0.01$, $^{*}P = 0.01$–0.05, $-P > 0.05$.

were separated into fibers subserving the inferior visual field and superior visual field. A comparative analysis was conducted between fibers projecting from the severely damaged retina compared with fibers projecting from the relatively preserved retina.

This study demonstrated for the first time a significant loss of fiber tracts in the corresponding part of the OR connected to the severely damaged part of the retina, while OR fibers connected to the relatively preserved retinal hemifield were spared. There was a 3-fold to 4-fold reduction in the number of fiber bundles projected to the affected hemifield compared with fibers projecting to the unaffected hemifield. Rarefaction of OR fibers in glaucoma has been reported previously.[14] This study, however, shows a topographical correspondence between RGC damage and loss of functionally connected OR fibers. Such evidence strengthens the case for secondary structural damage of the posterior visual pathway in glaucoma.

It is worth noting, however, that although OR fibers connected to the "unaffected" hemifield were spared, both OCT and visual field analysis still demonstrated a significant degree of RGC loss and reduction of visual field sensitivity, confirming early glaucomatous damage in this part of the nerve. Preservation of OR fibers projecting to the unaffected hemifield may relate to sensitivity of DTI or may suggest that axonal loss of LGN neurons occurs over a relatively long period of time, which has been reported in experimental literature looking at retrograde degeneration along the visual pathway.[21,22] Preservation of the "unaffected" fibers may also indicate that detectable axonal drop-out of LGN neurons occurs only after a certain threshold of RGC loss is reached, which may suggest a nonlinear nature of secondary transsynaptic degeneration.

The second novel finding of this study is that despite considerable differences in the degree of RGC damage between the affected and unaffected hemifields, some DTI parameters demonstrated similar abnormalities in both groups. Specifically, changes in RD and FA were not only seen in the remaining OR fibers projecting to the damaged retina, but also in the fibers connected to the RGCs of the relatively undamaged retina. Although there was a trend with a higher RD and MD in fibers projecting to the affected hemifield compared with those projecting to the unaffected hemifield, this difference did not reach statistical significance, with both regions abnormal. A higher average RD in glaucoma also has been recently demonstrated by another research group.[9,12]

In contrast to RD, AD, which represents axial flow, remained unchanged in both glaucoma and control groups, which explains both the reduction of FA and increase in MD in this study and is in agreement with previous reports.[7–10]

An increase in RD alone suggests that diffusivity in a direction perpendicular to axons is affected more than along axons in glaucoma. Radial diffusivity is thought to reflect the integrity of myelin sheaths, axonal cell membranes, and persistence of isotropic cells associated with gliosis, as previously shown in a rat model of fornix transection.[23] It can be argued that the increase in RD in glaucoma may represent underlying changes to these structures, such as demyelination, cell membrane loss, gliosis, or cytoskeletal changes, such as microtubule abnormalities. Although histological correlation with DTI is scarce, experimental animal models of multiple sclerosis have shown a relationship between perpendicular and parallel diffusivity with both demyelination and axonal loss[24] and more specifically between RD and myelin damage.[25,26] However there is no consensus on this issue, with one human postmortem multiple sclerosis study connecting myelin content with FA and MD changes.[27]

Further longitudinal studies using larger sample sizes are required to better assess the presence of transsynaptic degeneration and DTI metrics in pre-perimetric glaucoma. A larger sample size may identify differences in DTI indices between the glaucoma affected and unaffected groups. Correlation analyses may also be beneficial in eliciting a topographical relationship between RGC loss and OR changes in glaucoma of different severities. Although the automated DTI technique used in this study has shown to be reproducible and accurate, MRI resolution, movement artifact, and manual marking of the calcarine cortex may have limited the accuracy of DTI measurements. Furthermore, there is no consensus on DTI protocol in current literature, and diffusion tensor eigenvalues may not always represent pathological microstructure tissue changes.[28]

In summation, our analysis revealed a topographic relationship between RGC loss in glaucoma and damage to the posterior visual pathway. Significant changes of RD in preserved fibers of the OR suggest that DTI may assist in the evaluation of early glaucomatous damage in synaptically connected OR fibers.

Acknowledgments

Supported by National Health and Medical Research Council Grant 1056517.

Disclosure: **M. Kaushik**, None; **S.L. Graham**, None; **C. Wang**, None; **A. Klistorner**, None

References

1. Ono K, Hiratsuka Y, Murakami A. Global inequality in eye health: country-level analysis from the Global Burden of Disease Study. *Am J Public Health*. 2010;100:1784–1788.
2. Quigley HA, Broman AT. The number of people with glaucoma worldwide in 2010 and 2020. *Br J Ophthalmol*. 2006;90:262–267.
3. Gupta N, Yucel YH. Glaucoma as a neurodegenerative disease. *Curr Opin Ophthalmol*. 2007;18:110–114.
4. Yucel YH, Zhang Q, Weinreb RN, Kaufman PL, Gupta N. Atrophy of relay neurons in magno- and parvocellular layers in the lateral geniculate nucleus in experimental glaucoma. *Invest Ophthalmol Vis Sci*. 2001;42:3216–3222.
5. Gupta N, Ang LC, Noel de Tilly L, Bidaisee L, Yucel YH. Human glaucoma and neural degeneration in intracranial optic nerve, lateral geniculate nucleus, and visual cortex. *Br J Ophthalmol*. 2006;90:674–678.
6. Luthra A, Gupta N, Kaufman PL, Weinreb RN, Yucel YH. Oxidative injury by peroxynitrite in neural and vascular tissue of the lateral geniculate nucleus in experimental glaucoma. *Exp Eye Res*. 2005;80:43–49.
7. Chen Z, Lin F, Wang J, et al. Diffusion tensor magnetic resonance imaging reveals visual pathway damage that correlates with clinical severity in glaucoma. *Clin Exp Ophthalmol*. 2013;41:43–49.
8. Engelhorn T, Michelson G, Waerntges S, et al. A new approach to assess intracranial white matter abnormalities in glaucoma patients: changes of fractional anisotropy detected by 3T diffusion tensor imaging. *Acad Radiol*. 2012;19:485–488.
9. Engelhorn T, Michelson G, Waerntges S, et al. Changes of radial diffusivity and fractional anisotropy in the optic nerve and optic radiation of glaucoma patients. *ScientificWorldJournal*. 2012;2012:849632.
10. Garaci FG, Bolacchi F, Cerulli A, et al. Optic nerve and optic radiation neurodegeneration in patients with glaucoma: in vivo analysis with 3-T diffusion-tensor MR imaging. *Radiology*. 2009;252:496–501.
11. Michelson G, Engelhorn T, Waerntges S, Doerfler A. Diffusion tensor imaging for in vivo detection of degenerated optic radiation. *ISRN Ophthalmol*. 2011;2011:648450.
12. Michelson G, Engelhorn T, Warntges S, El Rafei A, Hornegger J, Doerfler A. DTI parameters of axonal integrity and demyelination of the optic radiation correlate with glaucoma indices. *Graefes Arch Clin Exp Ophthalmol*. 2013;251:243–253.
13. Zikou AK, Kitsos G, Tzarouchi LC, Astrakas L, Alexiou GA, Argyropoulou MI. Voxel-based morphometry and diffusion tensor imaging of the optic pathway in primary open-angle glaucoma: a preliminary study. *AJNR Am J Neuroradiol*. 2012;33:128–134.
14. Engelhorn T, Michelson G, Waerntges S, Struffert T, Haider S, Doerfler A. Diffusion tensor imaging detects rarefaction of optic radiation in glaucoma patients. *Acad Radiol*. 2011;18:764–769.
15. Sherbondy AJ, Dougherty RF, Ben-Shachar M, Napel S, Wandell BA. ConTrack: finding the most likely pathways between brain regions using diffusion tractography. *J Vis*. 2008;8(9):15.1–15.16.
16. Sherbondy AJ, Dougherty RF, Napel S, Wandell BA. Identifying the human optic radiation using diffusion imaging and fiber tractography. *J Vis*. 2008;8(10):12.1–12.11.
17. Sun HH, Wang D, Zhang QJ, Bai ZL, He P. Magnetic resonance diffusion tensor imaging of optic nerve and optic radiation in healthy adults at 3T. *Int J Ophthalmol*. 2013;6:868–872.
18. Chen WW, Wang N, Cai S, et al. Structural brain abnormalities in patients with primary open-angle glaucoma: a study with 3T MR imaging. *Invest Ophthalmol Vis Sci*. 2013;54:545–554.
19. You Y, Gupta VK, Graham SL, Klistorner A. Anterograde degeneration along the visual pathway after optic nerve injury. *PLoS One*. 2012;7:e52061.
20. Dai H, Morelli JN, Ai F, et al. Resting-state functional MRI: Functional connectivity analysis of the visual cortex in primary open-angle glaucoma patients. *Hum Brain Mapp*. 2013;34:2455–2463.
21. Cowey A, Alexander I, Stoerig P. Transneuronal retrograde degeneration of retinal ganglion cells and optic tract in hemianopic monkeys and humans. *Brain*. 2011;134:2149–2157.
22. Bridge H, Jindahra P, Barbur J, Plant GT. Imaging reveals optic tract degeneration in hemianopia. *Invest Ophthalmol Vis Sci*. 2011;52:382–388.

23. Stichel CC, Muller HW. Relationship between injury-induced astrogliosis, laminin expression and axonal sprouting in the adult rat brain. *J Neurocytol*. 1994;23:615–630.
24. Xu J, Sun SW, Naismith RT, Snyder AZ, Cross AH, Song SK. Assessing optic nerve pathology with diffusion MRI: from mouse to human. *NMR Biomed*. 2008;21:928–940.
25. Song SK, Sun SW, Ramsbottom MJ, Chang C, Russell J, Cross AH. Dysmyelination revealed through MRI as increased radial (but unchanged axial) diffusion of water. *Neuroimage*. 2002; 17:1429–1436.
26. Kim JH, Budde MD, Liang HF, et al. Detecting axon damage in spinal cord from a mouse model of multiple sclerosis. *Neurobiol Dis*. 2006;21:626–632.
27. Schmierer K, Wheeler-Kingshott CA, Boulby PA, et al. Diffusion tensor imaging of post mortem multiple sclerosis brain. *Neuroimage*. 2007;35:467–477.
28. Wheeler-Kingshott CA, Cercignani M. About "axial" and "radial" diffusivities. *Magn Reson Med*. 2009;61:1255–1260.

Investigative Ophthalmology & Visual Science